THE JOURNAL OF BIOLOGICAL CHEMISTRY VOL. 289, NO. 22, pp. 15384–15392, May 30, 2014

Reconciling the Structural Attributes of Avian Antibodies*

Received for publication, March 18, 2014, and in revised form, April 10, 2014 Published, JBC Papers in Press, April 15, 2014, DOI 10.1074/jbc.M114.562470

Paul J. Conroy[‡], Ruby H. P. Law[‡1], Sarah Gilgunn[§2], Stephen Hearty[¶], Tom T. Caradoc-Davies[‖], Gordon Lloyd[‡], Richard J. O'Kennedy[§¶2,3,4], and James C. Whisstock[‡1,3,5]

From the [‡]Department of Biochemistry and Molecular Biology, Faculty of Medicine, Nursing and Health Science, Monash University, Melbourne, Victoria 3800, Australia, [§]School of Biotechnology, Dublin City University, Dublin 9, Ireland, [¶]Biomedical Diagnostics Institute, National Centre for Sensor Research, Dublin City University, Dublin 9, Ireland, and [‖]Australian Synchrotron, 800 Blackburn Road, Clayton, Melbourne, Victoria 3168, Australia

Background: Antibodies from alternative immune hosts provide insights into novel mechanisms of antibody diversity in restricted germ-line repertoires.
Results: The high-resolution crystal structures of the first two chicken single chain antibodies (scFv) with prototypical binding sites are described.
Conclusion: Chickens exhibit unique canonical classes in the CDRL1.
Significance: Aves employ distinct mechanisms to generate diversity resulting in unique binding-site topologies.

Antibodies are high value therapeutic, diagnostic, biotechnological, and research tools. Combinatorial approaches to antibody discovery have facilitated access to unique antibodies by surpassing the diversity limitations of the natural repertoire, exploitation of immune repertoires from multiple species, and tailoring selections to isolate antibodies with desirable biophysical attributes. The V-gene repertoire of the chicken does not utilize highly diverse sequence and structures, which is in stark contrast to the mechanism employed by humans, mice, and primates. Recent exploitation of the avian immune system has generated high quality, high affinity antibodies to a wide range of antigens for a number of therapeutic, diagnostic and biotechnological applications. Furthermore, extensive examination of the amino acid characteristics of the chicken repertoire has provided significant insight into mechanisms employed by the avian immune system. A paucity of avian antibody crystal structures has limited our understanding of the structural consequences of these uniquely chicken features. This paper presents the crystal structure of two chicken single chain fragment variable (scFv) antibodies generated from large libraries by phage display against important human antigen targets, which capture two unique CDRL1 canonical classes in the presence and absence of a non-canonical disulfide constrained CDRH3. These structures cast light on the unique structural features of chicken antibodies and contribute further to our collective understanding of the unique mechanisms of diversity and biochemical attributes that render the chicken repertoire of particular value for antibody generation.

Antibodies are natural components of the vertebrate immune system produced by B-cells and function to identify foreign or "non-self" molecules. Due to their exquisite specificity, tune-able affinity, potency, stability, and ease of manufacturability antibodies have enjoyed enormous successes. The pharmaceutical industry has invested heavily in antibody-based therapeutics with 34 antibodies or antibody fragments approved worldwide, 28 of which are approved in both European and United States markets (1, 2), and an estimated 350 antibody-based therapeutics are in the clinical pipeline (2). Furthermore, antibody-based reagents are ubiquitous in diagnostic and research settings as valuable recognition tools. Although the pharmaceutical market is estimated to be worth more than forty billion U.S. dollars, diagnostic- and research-based antibody markets in 2012 were valued at eight billion and two billion, respectively.[6] Antibodies have come of age due to our increased understanding of their function, specificity, and origins. This collectively assembled knowledge-base draws observations from a number of disciplines including: structural biology, immunogenetics, cellular immunology, molecular biology, and bioinformatics (4). The three-dimensional structure of antibodies, both free and antigen-complexed, has played a central role in elucidating humoral immune response mechanisms, evolution of the antibody repertoire, and optimization of *in vitro*-generated antibodies (5). This has resulted in a number of powerful technological advances that have allowed protein engineers to actively harness and augment the potential of the immune system, including *in vitro* display technologies (6), humanization (7), and engineering of

* This work was supported by the Science Foundation Ireland (SFI) under Centres for Science Engineering and Technology (CSET) Grant 10/CE/B1821 (to P. J. C., S. H., and R. O. K.) and a SFI Short-term Travel Fellowship (to P. J. C.).

The atomic coordinates and structure factors (codes 4P48 and 4P49) have been deposited in the Protein Data Bank (http://wwpdb.org/).

[1] Supported by Australian Research Council and National Health and Medical Research Council grants.
[2] Supported by the Irish Cancer Society program Grant PCI11WAT, as part of the Prostate Cancer Research Consortium, Dublin, Ireland.

[3] Both are joint senior authors.

[4] To whom correspondence may be addressed: School of Biotechnology, Dublin City University, Dublin 9, Ireland. Tel.: 353-1-7007810; Fax: 353-1-7006558; E-mail: richard.okennedy@dcu.ie.
[5] An Australian Research Council Fellow and an Honorary National Health and Medical Research Council Principal Research Fellow. To whom correspondence may be addressed. Tel.: 61-4-18170585; Fax: 61-3-99029500; E-mail: james.whisstock@monash.edu.

[6] S. Yu, unpublished data.

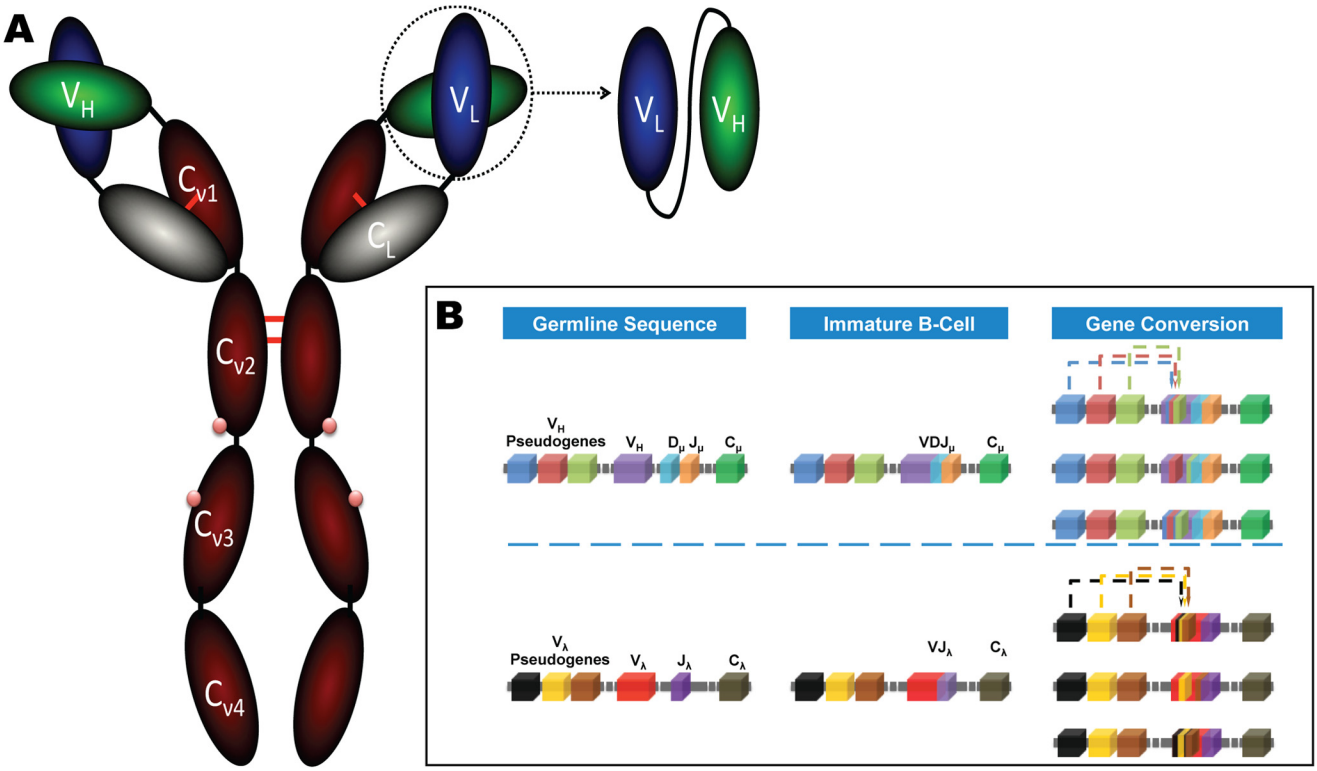

FIGURE 1. **Diagrammatic representation of antibody structure and the mechanism of gene conversion.** *A*, the IgY (180 kDa) from chicken is composed two identical polypeptide chains and, unlike IgG, has an additional constant heavy (*red*) domain and additional carbohydrate sites (*pink dots*). The single chain fragment variable (scFv) is constructed by isolation of the V_L (*blue*) and V_H (*green*) genes, which are linked in the V_L-V_H orientation by a flexible linker (*black line*). *B*, the process of gene conversion in chicken is depicted for both the heavy and light chain. In the H germ line, a functional V_H domain is composed of unique V_H and J_μ gene segments with one of a family of D_μ elements (~15). In the L germ line, only one light chain exists (λ), and every light chain is composed of the same V_λ-J_λ arrangement, which in itself generates minimal diversity. Interchromosomal gene conversion in immature B-cells gives rise to diversity by translocation of pseudogene sequences into the V-genes. Typically the closest pseudogene is used more frequently in gene conversion; however, in the light chain the pseudogenes are distributed across a 20-kb region preceding the V_L gene.

biophysical properties (*e.g.* affinity, functional activity, specificity) (4).

The natural immune repertoire is dynamic, with the capacity to generate a repertoire of 10^8 by affinity maturation *in vivo*, which is substantiated by continual exposure or sensitization to antigens from the environment or by immunization (8). Artificial manipulation of antibody genes has facilitated *in vitro* selection of truly unique antibodies from extremely large combinatorial libraries, which can be constructed from virtually any species, isolated from B-cells derived from naïve, immunized, or infected subjects or are partially or wholly synthesized *in vitro* (8). Display technologies such as phage, yeast, and ribosome display, when combined with high-throughput approaches for judicious library screening, have enabled the development of antibodies with highly tailored affinities, specificities, and biophysical properties (9, 10). The merits of *in vitro*-based antibody approaches, although largely under-appreciated by the research community, allow one to isolate antibodies with properties extremely or if not impossible to attain using the immune system alone (6, 8, 11). These powerful avenues of antibody development are of considerable importance for development of novel therapeutic entities and next generation diagnostic reagents and address the consternation among researchers arising from a preponderance of subpar research antibodies (12–14).

The specificity of antibodies is dictated by the hypervariable loops (15) or complementarity-determining regions (CDR)[7] (16) that form the sites for contact with its cognate antigen. The CDRs are described by canonical conformations, which are defined by the length of the hypervariable loop and both hypervariable loop/frame work region (FWR)-conserved residues (15). The FWR provides a structural scaffold for the antigen binding site and are important for structural diversity, the V_L/V_H orientation (4, 17) and in some instances may make direct antigen contacts. The IgY (Fig. 1*A*) is the typical low molecular weight antibody (180 kDa) of birds, amphibian, and reptiles and is considered to be the ancestral form of the mammalian IgG and IgE. Although similar to IgG, the IgY is structurally distinct (18) due to the presence of an additional constant heavy domain, lack of a *bona fide* hinge region, and differing oligosaccharide side-chain composition and, unlike IgG, is capable of eliciting anaphylactic mechanisms. As the hinge region is absent in IgY, its flexibility is derived from proline-glycine-rich regions at the Cν1-Cν2 and Cν2-Cν3 domains (18). At the genetic level, in contrast to humans, mice, and primates, the v-gene repertoire of chickens employs single functional v-genes for the heavy (V_H3 family) and light chains

[7] The abbreviations used are: CDR, complementarity determining region; cTnI, cardiac troponin I; FWR, frame-work region; PSA, prostate-specific antigen, scFv; single chain fragment variable; FC, flow cell.

(exclusively λ light chains), which contain unique V_L-J_L and V_H-D_H-J_H segments (19). In addition to somatic hypermutation, to generate a diverse functional antibody repertoire from such a restricted v-gene germ-line, chickens employ "gene conversion". This process is analogous to that in rabbits where each v-gene is significantly diversified by recombination of segments from upstream pseudogene blocks, which lack recombination signal sequences (Fig. 1*B*). As a consequence, the repertoire requires sequence homology between the germ line and pseudogenes to allow for donation of gene segments. Hence, a low level of FWR mutations was observed in V_H repertoire analysis coupled with maintenance of CDR structural residues, but modulation of those residues, which affect V_H/V_L interfaces (20). The chicken immune system can, therefore, introduce variability at selected FWR residues, resulting in structural diversity of V_H/V_L angles (4, 20). The D-segments of chickens (15 functional segments) are highly homologous, and hyperdiversification is achieved by gene conversion at D-D junctions, creating "mosaic CDRs" (19). These D-segments contain cysteine residues at a far higher frequency than humans or mice. This prevalence results in >50% of the chicken repertoire containing non-canonical CDRH3 cysteine residues and potentially plays an important role in functional diversity. Structures of such disulfide-containing CDRH3 across species are rare, as cysteine residues are observed at low frequency in mature B-cells (20). However, selection of avian CDRH3 non-canonical disulfide-containing clones from *Escherichia coli* indicates that it is possible to efficiently sample the full breadth of the chicken repertoire by phage display (19).

The use of chickens as diagnostic, and indeed therapeutic antibody generation hosts, is advantageous due to their phylogenetic distance from man, tolerance of multiple immunogens, and demonstrated successes in generating antibodies to a wide range of antigens (10, 19). Furthermore, the simplistic arrangement of v-genes, high core temperature, and increased CDRH3 length provide potentially superior antibody biophysical attributes. The unique properties of chicken antibodies have been demonstrated experimentally and are illustrated by detailed repertoire analysis. However, few investigations have examined the structural basis of these attributes to explain the demonstrated functional biology. In this study we have resolved the high resolution crystal structures of two unique chicken antibodies, selected from protein- and peptide-immunized repertoires by phage display, with nanomolar and picomolar affinity (10). The crystal structures have revealed unique topologies and arrangements within the CDRs of chicken antibodies that contribute our increased understanding of antibody diversity.

EXPERIMENTAL PROCEDURES

Antibody Selection—The single chain fragment variable (scFv) libraries were generated in the V_L-V_H orientation, as described by Andris-Widhopf *et al.* (21). Clone 180 was selected from a cardiac Troponin I (cTnI) peptide (^{39}KISASRKLQLKT^{50})-immunized repertoire by iterative cycles of phage display, as described previously (10). Clone B8 was selected from a PSA protein (human seminal fluid; SCIPAC)-immunized repertoire. Briefly, an adult leghorn was immunized with PSA, sacrificed, and the antibody repertoire was accessed from mRNA isolated from B-cells (femur bone marrow and spleen tissue) and displayed on the surface of filamentous phage (21). The antibody was isolated by iterative cycles phage display with increasing stringency exerted by serial limitation of adsorbed PSA.

Antibody Expression and Purification—ScFv antibodies were expressed within the periplasmic space of *E. coli* Top10F′ (Invitrogen) with the pComb3x vector (21). Single colonies were selected from LB-agar supplemented with 25 μg/ml carbenicillin and grown overnight in 5 ml of Superbroth supplemented with 25 μg/ml carbenicillin and 1% (w/v) glucose at 37 °C with shaking at 220rpm. This starter culture was used to inoculate 100 ml of Superbroth with 25 μg/ml carbenicillin and was grown to A_{600} = ~0.6 before subculturing into 10 × 500 ml of Superbroth with 25 μg/ml carbenicillin (2-liter flasks). At A_{600} = ~0.6, the cultures were induced with 0.2 mM isopropyl 1-thio-β-D-galactopyranoside at 30 °C with shaking at 230 rpm overnight (~16 h). The bacteria were harvested by centrifugation (3220 × *g*) at 4 °C for 20 min. Soluble scFv were released from the periplasmic space by osmotic shock in a two-step process. The pellet was first thoroughly resuspended in 1× TBS (25 mM Tris, pH 8.0, 150 mM NaCl), and an equal volume of 2× shock buffer (50 mM Tris, pH 8.0, 300 mM NaCl, 1 M sucrose, and 2 mM EDTA) was added before incubation at room temperature for 15 min. Shocked cells were recovered by centrifugation (12,400 × *g* at 4 °C for 20 min) followed by resuspension in ice-cold 5 mM $MgSO_4$ and incubation on ice for 15 min. The periplasmic-stripped cells were collected by centrifugation (27,200 × *g* at 4 °C for 20 min), and 0.2 times the volume of 5× binding buffer (125 mM Tris, pH 8.0, 750 mM NaCl, 50 mM imidazole, 0.02% NaN_3) was added to the supernatant. HisBind (Novagen) resin (1 ml equilibrated in 30 ml of 1× binding buffer) was added, and scFv was recovered by batch binding for 2 h at 4 °C on an end-over-end roller. The resin was collected by gravity flow and washed with 30 ml of binding buffer followed by a second wash with 30 ml of wash buffer (25 mM Tris, pH 8.0, 150 mM NaCl, 20 mM imidazole, 0.05% (v/v) Tween® 20, 0.02% NaN_3). Bound protein was eluted with 7–10 ml of elution buffer (1× running buffer, 300 mM imidazole) in 0.5-ml fractions, and protein-containing fractions were pooled and concentrated to 2 ml in a 3-kDa concentrator (Merck-Millipore). The pooled fractions were resolved by size exclusion chromatography (S75 16/60; GE Healthcare) in 25 mM Tris, pH 7.4, 150 mM NaCl, 0.02% NaN_3. The purified protein was analyzed by SDS-PAGE and Western blot.

Affinity Measurement—Both scFvs were analyzed by surface plasmon resonance-based kinetic evaluation in a hemagglutinin (HA) epitope-capture approach. An anti-HA monoclonal antibody (Thermo Fisher Scientific) was immobilized by 1-ethyl-3-(3-dimethylaminopropyl)carbodiimide (EDC)-*N*-hydroxysuccinimide (NHS) (GE Healthcare) coupling on the surface of a CM5 chip (GE Healthcare) and capped with 1 M ethanolamine (10, 22). ScFv 180 was analyzed on a Biacore™ 4000 (GE Healthcare) using serial dilutions (12 to 0.19 nM) of purified human cTnI (Life Diagnostics) in HBS-EP$^+$ (GE Healthcare) at 25 °C. ScFv B8 was analyzed on a Biacore™ 3000 (GE Healthcare) using serial dilutions of purified human PSA (12.5 to 0.39 nM) in a method described previously (22). The data were col-

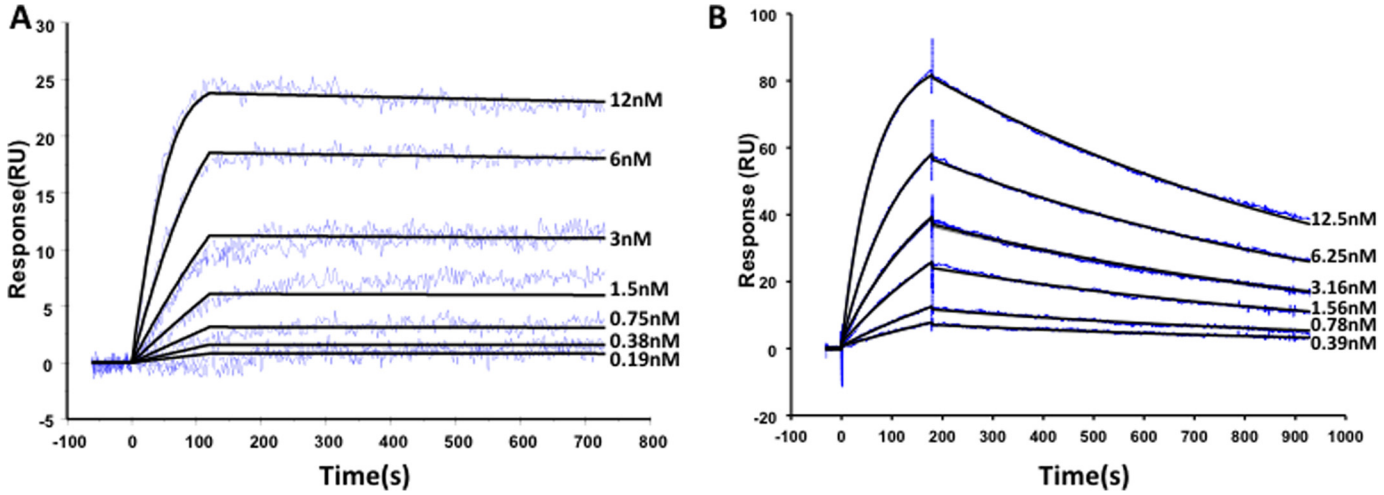

FIGURE 2. **Kinetic evaluation of the avian scFvs with their respective protein antigens.** Both scFv were analyzed in a HA capture configuration, which oriented the scFv on the surface of the sensor chip. *A*, scFv180 was analyzed on a Biacore 4000™. The flow cell (FC) contained 5 spots; spots 1 and 5 were active (anti-HA + scFv + cTnI), spots 2 and 4 were control spots (anti-HA + cTnI), and spot 3 was an activated-deactivated surface control. Each was independently monitored, the sensorgrams double reference-subtracted (spot 1–2 and 5–4 and a buffer only control), and the 3 nM concentration was carried out in duplicate. *B*, scFvB8 was analyzed on a Biacore 3000™. FC 1 and 2 were functionalized with the anti-HA capture antibody. Purified scFv was captured on FC 2 only and PSA passed over FC 1 and 2. The sensorgrams were FC2–1 and double (buffer) reference-subtracted, and the 3.16 nM concentration was carried out in duplicate. Three independent analyses were carried out, and kinetic constants are reported ± standard error (Table 1). *RU*, response units.

lected and processed using the dedicated Biaevaluation software (GE Healthcare). The data were double-referenced by subtraction of a "buffer only" control against the reference cell/spot-subtracted sensorgrams.

Crystallization—ScFv 180 and scFv B8 were concentrated to 16 and 5.8 mg/ml, respectively, with a 3-kDa concentrator (Merck-Millipore). Crystallization was carried out by the hanging drop method with a 1:1 mixture of protein and mother liquor at 4 °C, where crystals formed in 3–7 days. Initial crystal-forming conditions were identified from the Basic Crystallization kit for Proteins (Sigma). After refinement of the conditions, crystals of scFv 180 were obtained in 0.1 M Tris-HCl, pH 9.6, 0.2 M NaOAc, 29% (w/v) PEG 4000 with 0.1 M glycine. Crystals of scFv B8 were obtained in 0.1 M NaOAc, pH 4.6, 0.2 M ammonium sulfate. The crystals were flash-cooled in liquid nitrogen using 25% (v/v) glycerol as the cryoprotectant.

Structure and Refinement—Data sets were collected at the Australian Synchrotron MX2 beamline at 100K (23). The data were merged and processed using XDS (24), POINTLESS, and SCALA (25). Five percent of the data set was flagged as a validation set for calculation of the R_{free}. Molecular replacement of scFv 180 was carried out using PDB code 1MCP as a search probe. Molecular replacement was carried out with the hypervariable loops removed and initially with the light chain only followed by the heavy chain with the light chain fixed. One molecule was found per asymmetric unit cell, and an initial model was generated using wARP (26). Model building was performed using COOT (27), and refinement was performed using PHENIX (28) and REFMAC (29). Molecular replacement of scFv B8 was carried out using scFv 180 as a model, and one molecule was found in the asymmetric unit. The starting model, model building, and refinement were carried out as for scFv 180. Crystallographic and structural analysis was performed using CCP4 suite (30) unless otherwise specified. Secondary structure assignment was carried out using STRIDE (31). The figures were generated using PyMOL (32), and the structural validation was performed using MolProbity (33). All atomic coordinates and structural factors were deposited in the PDB under codes 4P48 (scFv 180) and 4P49 (scFv B8).

TABLE 1
SPR kinetic analysis of scFvs

scFv	k_a	k_d	K_D
	$M^{-1}s^{-1}$	s^{-1}	
B8	$1.07 \pm 0.16 \times 10^6$	$1.07 \pm 0.03 \times 10^{-5}$	1.01 ± 0.12 nM
180	$2.29 \pm 0.97 \times 10^6$	$4.07 \pm 1.63 \times 10^{-5}$	17.97 ± 0.96 pM

RESULTS

The antibody fragments were selected from V_L-V_H-orientated libraries constructed from high-titer chicken immunization regimens using both peptide (scFv 180)- and native protein-based (svFv B8) immunogens. In both cases the scFvs were selected by iterative cycles of phage display against purified human proteins (data not shown) (10).

Binding Analysis—Detailed kinetic analysis (Fig. 2) was carried out using surface plasmon resonance technology in a capture approach. The pComb3x-encoded HA tag facilitated oriented capture of highly functional antibody surfaces with the binding responses monitored with the protein antigen as ligands. Both scFvs were found to interact with their respective antigens with high affinity (Table 1). The selection approach applied to scFv 180 (10) was tailored to ensure that the kinetics were suited to a room temperature, point-of-care (POC) device, and therefore, its rapid association (k_a) was expected to perform optimally in a short assay time frame, and once bound, its slow dissociation constant (k_d) gave rise to particularly high affinity antibody in the low picomolar range (18 pM; Table 1). In analysis, using the cognate peptide conjugated to a carrier protein, the affinity was found to be ~5-fold lower (99 pM; data not shown). ScFv B8 exhibits classical single digit nanomolar affinity (1 nM) associated with *in vivo*-matured antibodies.

Sequence Analysis—Alignment of the V_L, V_H, and germ-line sequences (Fig. 3) illustrates the typical FWR sequence uni-

FIGURE 3. **Amino acid alignment of avian scFv and germ-line sequence.** The chicken scFvs were numbered by the Chothia, Chothia with structurally corrected framework indels, and Kabat schemes. The framework regions (*FR*) and CDRs are indicated *below the numbering schemes*, with the associated CDR definitions for each scheme indicated by the *red-shaded areas*. Variations in amino sequence from the germ-line (for scFv 180 and B8) are highlighted in *gray* for clarity, insertions are indicated by the *yellow boxes*, and *gaps* are illustrated by *dashes*. The sequences of the V_L and V_H of the avian Fab PDB code 4GLR are shown at the *bottom* for comparison (19). The chicken mature light chain is two residues shorter than that of the typical mammalian λ light chain and, therefore, begins at position number *3*. The antibodies were numbered using "Abysis" (53).

formity observed in chicken antibodies. Within the FWR of the V_L, mutations occurred at residues L17 and L20 (scFv 180 only) and at Vernier positions L47 and L71 (scFv B8 only). In the V_H, mutations were observed at Vernier positions H2 (scFv 180 only), H47 (light chain contact residue), and H78. Within the V_L CDRs, scFv 180 exhibits a high level of CDRL1 diversification with a significant insertion of aromatic (Tyr), small (Gly), and charged (Arg) amino acids, resulting in a 14-residue CDRL1 (Kabat definition unless otherwise stated; see Fig. 3), which correlates with a recent study where CDRL1 canonical structure distribution could differentiate antibodies for specific antigens (proteins, peptides, and haptens) (4, 5). Anti-peptide binding antibodies tend to favor longer CDRL1 loops (11–13) over the shorter loops observed within anti-protein binding antibodies (6–8 residues) (5). The antibodies have similar CDRH1; however, the CDRH2 are significantly diversified, containing small (Gly/Ser), negatively charged (Asp), hydrophobic (Ile), and aromatic (Tyr) residues. Unsurprisingly, the two scFv have highly divergent sequence composition of the CDRH3, and furthermore, exhibit a differing residue composition of the paratope when compared with humans and mice (20). In both cases the CDRH3 are biased toward small amino acids (Gly/Ser/Ala/Cys) with a low frequency of Tyr, which is the dominant residue of mice and humans (4). Both CDRs maintain the conserved residues Lys/Arg-94 and Asp-101 of the theoretical bulged/kinked CDR (34, 35), which appears to hold true for the majority but not all structures (36). The CDRH3 of scFv 180 is 15 residues long, dominated by small (Gly and Ser), negatively charged (Asp) residues with a single aromatic (Tyr) residue. The CDRH3 of scFv B8 is 14 residues long, composed of small (Gly/Ser/Ala/Cys), positive (His/Arg), and hydrophobic (Ile/Leu) residues. It is of the chicken V_H major structural class type 1, due to the pair of non-canonical cysteine residues (^{94}ARSH-*CSGCR*NAALIDA^{102}), as defined by Wu *et al.* (20).

Crystal Structure—To investigate the structural attributes of avian fragments, crystal screening was undertaken. The scFvs were purified to homogeneity from the periplasmic space of *E. coli* in a two-step purification protocol and were concentrated to 16 mg/ml (scFv 180) and 5.8 mg/ml (scFv B8) for x-ray crystallography. The resultant structures were solved at high resolution (Table 2): 1.35 Å in the *P2* space group for scFv 180 and 1.40 Å in the *P6* space group for scFv B8. In both cases there was a single molecule in the asymmetric unit. The two structures illustrate the prototypical binding site topologies for anti-peptide and anti-protein binding antibodies. The long CDRL1 and CDRH3 of scFv 180 created a protruding binding site (Fig. 4*B*) with a groove at the center (Fig. 4*C*), which is the classical anti-peptide binding antibody topology (4). Electrostatic surface analysis of the scFv shows a negatively charged binding site (Fig. 4*D*). In contrast, anti-protein antibodies tend to have larger, flat binding sites, and the prototypical topology was observed in the scFv B8 structure (Fig. 4, *B* and *C*) where the electrostatic surface reveals a predominantly positively charged

TABLE 2

Refinement statistics

Highest resolution shell is shown in parentheses. ASU, asymmetric unit.

	scFv 180 (4P48)	scFv B8 (4P49)
Data Collection		
Resolution range (Å)	19.79-1.35 (1.398-1.35)	50.40-1.40 (1.45-1.40)
Space group	$P2_1\,2_1\,2_1$	$P6_1\,2\,2$
a, *b*, *c* (Å)	51.78, 58.379, 69.048	52.46, 52.46, 302.38
α, β, γ (°)	90, 90, 90,	90, 90, 120
Unique reflections	46,638 (4,575)	49,948 (4,592)
Completeness (%)	99.97 (99.74)	99.39 (94.19)
Multiplicity	7.9 (7.5)	17.7 (9.1)
$\langle I\rangle/\langle\sigma(I)\rangle$	14.57 (3.90)	48 (2.17)
Wilson B-factor (Å^2)	9.74	14.98
R-merge (%)	0.085 (0.453)	0.126 (0.910)
R_{pim} (all I+ and I−)	0.032 (0.174)	0.029 (0.313)
R_{meas} (all I+ and I−)	0.091 (0.486)	0.129 (0.964)
Refinement		
Number of molecules in ASU	1	1
Resolution Limit (Å)	1.35	1.40
R-work	0.1560 (0.1944)	0.1829 (0.2860)
R-free	0.1759 (0.2263)	0.2138 (0.3348)
Number of atoms	2,144	2,036
Macromolecules	1,783	1,681
Ligands		24
Water	361	331
Protein residues	235	226
Root mean square deviations		
Bond lengths (Å)	0.01	0.006
Bond angles (°)	1.27	1.02
Ramachandran plot		
Favored (%)	99	98
Outliers (%)	0	0
Clashscore (Molprob)	1.75	3.02
Average B-factor	10.3	23.0
Macromolecules	7.9	20.2
Ligands		44.40
Solvent	21.8	35.70

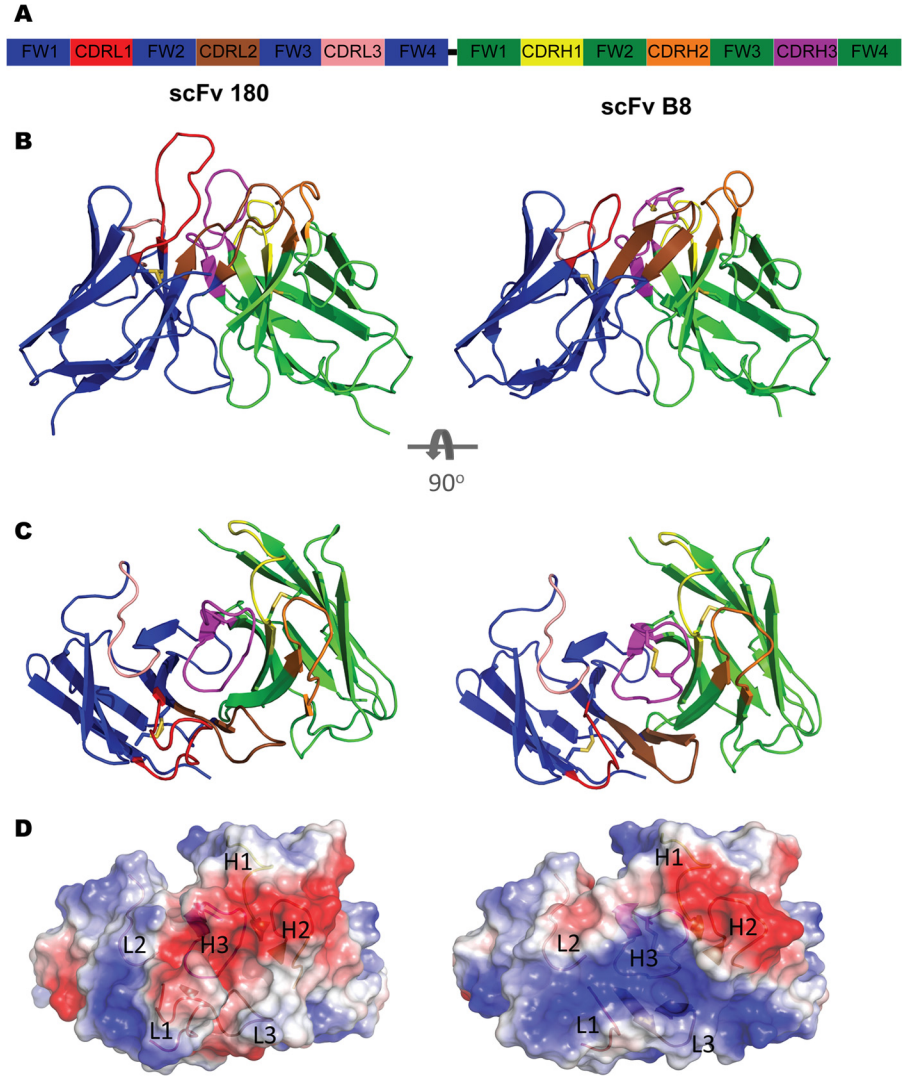

FIGURE 4. **Structures of scFv 180 and B8.** *A*, diagrammatic representation of the scFv format colored by chain (V_L, *blue*; V_H, *green*) with the CDR L1 (*red*), L2 (*salmon*), L3 (*brown*), H1 (*yellow*), H2 (*orange*), and H3 (*magenta*) shown. The flexible linker (*black*) connects the C terminus of the V_L to the N terminus of the V_H but was not modeled in the solved structure. *B*, ScFv 180 is dominated by the CDRL1 and H3, which protrudes into the solvent, creating a grooved binding site that is typical of an anti-peptide antibody. The CDR arrangement of scFv B8 is more compact creating a "shelf-like" arrangement for antigen binding. *C*, the antibody binding sites as viewed from the antigen perspective. *D*, the transparent electrostatic surface view of the scFvs, from the antigen perspective, with the CDR loops visible. The positively and negatively charged areas are indicated in *blue* and *red*, respectively. ScFv 180 has a predominantly negatively charged pocket that is largely attributed to CDRs L1 and H3. In contrast, scFv B8 has a predominantly positively charged surface.

binding site (Fig. 4*D*). As these two structures represent two of only three chicken structures available, a comparison of human and murine canonical CDRs, as classified by North *et al.* (36), was undertaken. Alignment of the two scFv with the chicken Fab (PDB code 4GLR) shows significant FWR sequence similarity (Fig. 5*A*). The chicken CDRs L2, L3, H1, and H2 comply with canonical conformations seen in mammalian structures. ScFv 180 could be classified into the clusters L2–8, L3–11, H1–13, H2–10. ScFv B8 was classified into the clusters L2–8, L3–9, H1–13, and H2–10; although the CDRH2 length was 11 residues, the structural class was well matched. In the case of both antibody structures, the CDRH3 adopted the kinked/bulged conformations of the torso, and the CDRL1 had canonical conformations that are distinct from all clusters described in human and rodents to date. The CDRL1 of scFv B8 matches the unique canonical conformation described by Shih *et al.* (19) for the chicken anti-pTau antibody (PDB code 4GLR) (Fig. 5*B*). The two non-canonical cysteine residues in the CDRH3 of scFv B8 form a disulfide within the CDRH3 and appear to support the adjacent, positively charged His-96 and Arg-100A residues. This bonding appears at a high frequency number of other species including camelids, sharks, cows, pigs, and platypus (4), where the rigidity imparted by these disulfide bonds to long loops may be advantageous by minimizing entropic penalties during binding events (37) and have been shown to be essential for stability and binding function (data not shown) (38). This is the second example of such a CDRL1 canonical class that appears to be unique to chicken and was observed in crystal structures of two avian antibodies with intra-CDRH3 disulfide bonds (Fig. 5*B*). Although both of these chicken structures show this unique binding site arrangement, the nature of the antigens bound by the topology is different (PDB code 4GLR is phosphopeptide binding, and scFv B8 is protein binding). It would, therefore, appear that the mechanism is not implicitly

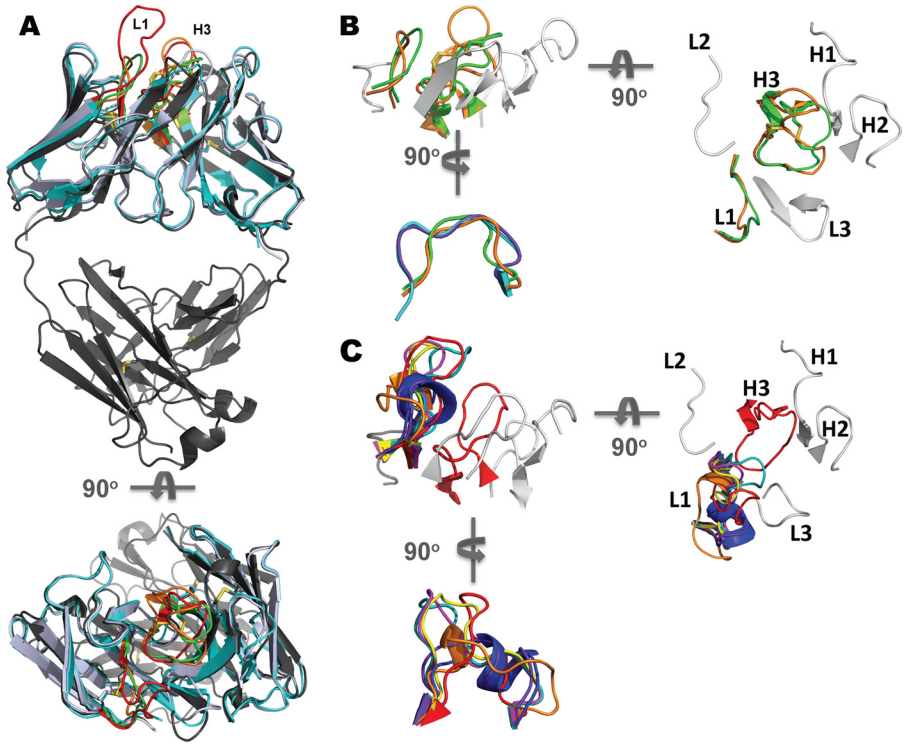

FIGURE 5. **Uniquely chicken CDRL1 canonical structures.** *A*, schematic view of avian scFv 180 (*blue-white*), B8 (*cyan*), and Fab PDB code 4GLR (*gray*) illustrating the degree of structural similarity of the avian variable domains. The view is rotated through 90° (below) to view the antibodies from the antigen perspective. In both views, the CDRL1 and H3 are highlighted for each avian antibody: scFv 180 (*red*) scFvB8 (*green*), Fab PDB code 4GLR (*orange*). *B*, schematic view (as in *A*) illustrating the CDR arrangement of scFv B8. The CDRL1 and H3 (*green*) are overlaid with PDB code 4GLR (*orange*) with the remainder of the CDRs colored in *gray*. The CDRs are labeled on the view rotated through 90° to view the CDR arrangement from the antigen perspective (*right*) showing the non-canonical cysteine residues (Cys-97 and Cys-100) that form the intra-CDRH3 disulfide bond. The schematic view rotated through 90° of the avian scFv B8 CDRL1 (*bottom*) aligned and superimposed onto the median canonical mammalian clusters, CDRL1-10-1 (PDB code 1YQV: L, *cyan*), CDRL1-10-2 (PDB code 1AY1, L, *purple*), and the avian anti-pTau Fab (PDB code 4GLR: I, *orange*). The scFv B8 L1 is eight residues in length (24–34) and does not match any of the canonical clusters defined by North *et al.* (36); however, it does share a canonical structure with that of the chicken Fab, PDB code 4GLR. *C*, schematic view of scFv180 CDRL1 and H3 (*red*, in the same view as *A*) with the light chain aligned with representative structures of the canonical mammalian CDRL1 clusters. The CDRs are labeled on the view rotated through 90° to view the CDR arrangement from the antigen perspective (*right*). The view is rotated 90° to view the CDLR1 canonical structure alignment (*bottom*) where the CDRL1 (*red*) is superimposed onto the canonical mammalian clusters: CDRL1–13-1 (*blue*; PDB code 2A9M), CDRL1–14-1 (*orange*; PDB code 1NC2), CDRL1–14-2 (*purple*; PDB code 1DCL), CDRL1–15-1 (*magenta*; PDB code 1EJO), CDRL1-15-2 (*yellow*; PDB code 1I7Z) and CDRL1–16-1 (*teal*; PDB code 2D03). The scFv 180 CDRL1 is 14 residues in length (residues 24–34); however, it is not represented in the L1–14-1 cluster as defined by North *et al.* (36). The closest structural representative loop conformation is that of the murine anti-glycophorin A κ-light chain (PDB code 2D03; *teal*), which belongs to the L1–16-1 cluster.

antigen type-specific, although the binding site topology of PDB code 4GLR does not possess a typical "grooved" paratope associated with peptide binding antibodies because of the "bowl-like" recess in the CDRH2 that accommodates the phosphate group (19). In the case of scFv B8 CDRH2, the tyrosine residue at position H56 fills this recess, and the CDRH3 is flatter, with small amino acids directed toward the CDRH2 within the disulfide-bonded loop, which anchors two positively charged residues (His-96 and Arg-100A) positioned either side of the loop. This is in contrast to PDB code 4GLR, where the disulfide bond is positioned to hold the CDRH3 in such a conformation as to position the phosphothreonine (Thr(P)-231) in contact with the bowl-like recess in CDRH2 through orientation of key CDRH3 antigen-contacting residues (19). The scFv 180 CDRL1 (^{24}SGGGRYYDGSYYYG^{34}) is 14 residues in length composed of small (Gly/Ser; 50%), hydrophobic (Tyr; 35.7%) and charged residues (Arg/Asp; 14.3%). The long loop is stabilized by a network of inter- and intra-CDR contacts and contacts with both the LFR and HFR. Its length groups it in CDRL1–14 cluster; however, a structural comparison with light chains of the CDRL1–14-1 and CDRL1–14-1 median structures, PDB codes 1NC2 and 1DCL, indicated that it adopts an extended loop conformation (Fig. 5*C*). Furthermore, the loop appears to be more structurally similar to the extended loops of the longer clusters CDRL1–15-1 (PDB code 1EJO), L1–15-2 (PDB code 1I7Z), and L1–16-1 (PDB code 2D03) when aligning the CDRL1 loops only, independent of FWR (data not shown). The long CDRH3 (16 residues, North *et al.* (36), CDR definition) contains small (Gly/Ser; 43.75%), hydrophobic (Ala/Ile/Tyr; 25%), and charged residues (Asp/Lys; 31.25%) forming a grooved pocket with the CDRL1 (Fig. 4, *B* and *C*), which is negatively charged (Fig. 4*D*) and would appear to be a logical outcome given the highly charged nature of both cTnI (pI = 9.87) and the peptide (pI = 11.26) at physiological pH. The crystal structure of cTnI (PDB code 1J1D) indicates that this N-terminal region is α-helical and strongly positively charged. This antibody, although raised against a linear synthetic peptide, also recognizes epitope in the context of the native protein (Fig. 2 and Table 1) as previously described (10). It is likely that the peptide immunogen adopted a conformation to mimic this helical region or the binding event with the antibody causes the peptide to adopt a mimic conformation, and a recent study suggests that key "anchor" residues in the C terminus of such peptides are responsible for peptide specificity of antibodies and other peptide-binding proteins (39).

DISCUSSION

In chicken, as in higher vertebrates, the primary mechanism for V_H diversification is V-D-J recombination and somatic hypermutation (20, 40, 41). However, the chicken V_H repertoire is diversified by gene conversion in place of a diverse repertoire of sequences/structures, whereby multiple upstream pseudogenes can undergo recombination into the V_H gene after functional V-D-J rearrangements. This mechanism leads to both mutation of the CDRs and modulation of the FWR (20). The chicken antibody repertoire has been extensively examined at the genomic level and also in terms of both functional isotype content (4, 42). Recently, a number of studies have exploited the chicken repertoire to generate high quality antibodies to a wide range of antigens (10, 19, 22, 43–48), have extensively examined the characteristics of the repertoire with detailed analysis of amino acid diversity in both naïve and selected repertoires (20), and have presented the crystal structure of an chicken Fv domain (19).

This study presents two high affinity chicken scFv crystal structures with prototypical binding site topologies for peptide and protein antigen binding. The antibodies were generated from immunized repertoires by phage display and interacted with their cognate antigens with high affinity (scFv B8, 1 nM; scFv 180, 20 pM). These antibodies exemplify the power of display technologies, in particular phage display, to not only recapitulate (scFv B8) but also exceed (scFv 180) the diversity of host immune system to generate antibodies that surmount the theoretical affinity ceiling (8, 49). Combinatorial libraries facilitate combinations of heavy and light chains that are truly randomized, not represented or accessible in the natural B-cell repertoire, and routinely permit isolation of antibodies with sub-single digit nanomolar affinities (8). Thus, such technologies facilitate exploitation of the true affinity potential of the natural repertoire *in vitro*.

The structures revealed a number of interesting canonical structural grouping deviations that may well be distinctly "chicken." At present the paucity of chicken structures in the Protein Data Bank precludes a rational, focused appraisal of the consequences of novel CDRL1 canonical structures or the non-canonical disulfide-bonded CDRH3 for the classical modes of protein, peptide, or hapten binding. The CDRL1 of scFv B8 mirrors the chicken canonical cluster described by Shih *et al.* (19), and its presence is also concurrent with a long, non-canonical disulfide-constrained CDRH3, which exhibits a distinct bias toward small amino acids (Gly/Ser/Ala/Cys/Thr) (4, 20). This may suggest that such a binding site arrangement is not antigen binding mode-specific but raises the possibility that it is necessary to have a short CDL1 to facilitate the elongated and disulfide constrained CDRH3. These descriptive structures further support the increasing genetic, functional, and now structural evidence that such constrained CDRH3 is an active diversification strategy in the restricted germ-line repertoire of chicken (19, 20). This CDRL1-CDRH3 arrangement forms a common structure in chicken antibodies (two of the three available chicken structures) that is distinctly different from the structures described in mammals to date (19, 36, 50). Furthermore, the CDRL1 of scFv 180 also exhibits a conformation that has not been observed to date in humans and rodents, which is distinct from those observed for both scFv B8 and PDB code 4GLR, which forms an extended CDRL1 and is the basis of a grooved peptide binding paratope in combination with a long CDRH3.

The selection of an avian CDRH3 with non-canonical disulfides from *E. coli* demonstrates not only the capacity to fully access the chicken repertoire but the importance of including such mechanisms of diversity in selection of novel antibody candidates (19, 51). The restricted v-gene germ-line repertoire in chicken has evolved mechanisms capable of achieving equivalent levels of Ig protection but is distinct from murine, human, and primate mechanisms and is fully capable of broad range antigen recognition (20). Therefore, chicken antibodies present a valuable reservoir of antibodies that could be tapped into for superlative diagnostics and possibly therapeutic entities.

The recent crystal structures of chicken (described here and by Shih *et al.* (19)) and bovine (52) antibodies have revealed unique and even surprising mechanisms to generate diversity within the immunoglobulin fold often with restricted germ-line repertoires. Accruing knowledge of antibody structure, function, repertoire, and origin is crucial for a number of important applications including man-made, knowledge-based, repertoire synthesis, and antibody-based drug discovery. These structures give structural endorsement to the active mechanisms of diversification employed by the chicken repertoire by highlighting two descriptive examples of uniquely chicken antibody structures.

Acknowledgments—We acknowledge the infrastructure support from Monash University platforms: Protein Production, Biomedical Proteomics, and Macromolecular Crystallization. This research was undertaken on the MX2 beamline at the Australian Synchrotron, Victoria, Australia.

REFERENCES

1. Reichert, J. M. (2012) Marketed therapeutic antibodies compendium. *MAbs* **4,** 413–415
2. Reichert, J. M. (2013) Which are the antibodies to watch in 2013? *MAbs* **5,** 1–4
3. Deleted in proof.
4. Finlay, W. J., and Almagro, J. C. (2012) Natural and man-made V-gene repertoires for antibody discovery. *Front. Immunol.* **3,** 342
5. Raghunathan, G., Smart, J., Williams, J., and Almagro, J. C. (2012) Antigen-binding site anatomy and somatic mutations in antibodies that recognize different types of antigens. *J. Mol. Recognit.* **25,** 103–113
6. Bradbury, A. R., Sidhu, S., Dübel, S., and McCafferty, J. (2011) Beyond natural antibodies: the power of *in vitro* display technologies. *Nat. Biotechnol.* **29,** 245–254
7. Safdari, Y., Farajnia, S., Asgharzadeh, M., and Khalili, M. (2013) Antibody humanization methods: a review and update. *Biotechnol. Genet. Eng. Rev.* **29,** 175–186
8. Hearty, S., and O'Kennedy, R. (2011) Exploiting recombinant antibodies in point-of-care (POC) diagnostics: the combinatorial advantage. *Bioeng. Bugs* **2,** 182–186
9. Conroy, P. J., Hearty, S., Leonard, P., and O'Kennedy, R. J. (2009) Antibody production, design, and use for biosensor-based applications. *Semin. Cell Dev. Biol.* **20,** 10–26
10. Conroy, P. J., O'Kennedy, R. J., and Hearty, S. (2012) Cardiac troponin I: a case study in rational antibody design for human diagnostics. *Protein Eng. Des. Sel.* **25,** 295–305
11. Lerner, R. A. (2006) Manufacturing immunity to disease in a test tube: the magic bullet realized. *Angew. Chem. Int. Ed. Engl.* **45,** 8106–8125
12. Saper, C. B. (2005) An open letter to our readers on the use of antibodies. *J. Comp. Neurol.* **493,** 477–478

13. Bordeaux, J., Welsh, A., Agarwal, S., Killiam, E., Baquero, M., Hanna, J., Anagnostou, V., and Rimm, D. (2010) Antibody validation. *Biotechniques* **48,** 197–209
14. Colwill, K., Renewable Protein Binder Working Group, and Gräslund, S. (2011) A roadmap to generate renewable protein binders to the human proteome. *Nat. Methods* **8,** 551–558
15. Chothia, C., and Lesk, A. M. (1987) Canonical structures for the hypervariable regions of immunoglobulins. *J. Mol. Biol.* **196,** 901–917
16. Wu, T. T., and Kabat, E. A. (1970) An analysis of the sequences of the variable regions of Bence Jones proteins and myeloma light chains and their implications for antibody complementarity. *J. Exp. Med.* **132,** 211–250
17. Abhinandan, K. R., and Martin, A. C. (2010) Analysis and prediction of VH/VL packing in antibodies. *Protein Eng. Des. Sel.* **23,** 689–697
18. Warr, G. W., Magor, K. E., and Higgins, D. A. (1995) IgY: clues to the origins of modern antibodies. *Immunol. Today* **16,** 392–398
19. Shih, H. H., Tu, C., Cao, W., Klein, A., Ramsey, R., Fennell, B. J., Lambert, M., Ní Shúilleabháin, D., Autin, B., Kouranova, E., Laxmanan, S., Braithwaite, S., Wu, L., Ait-Zahra, M., Milici, A. J., Dumin, J. A., LaVallie, E. R., Arai, M., Corcoran, C., Paulsen, J. E., Gill, D., Cunningham, O., Bard, J., Mosyak, L., and Finlay, W. J. (2012) An ultra-specific avian antibody to phosphorylated tau protein reveals a unique mechanism for phosphoepitope recognition. *J. Biol. Chem.* **287,** 44425–44434
20. Wu, L., Oficjalska, K., Lambert, M., Fennell, B. J., Darmanin-Sheehan, A., Ní Shúilleabháin, D., Autin, B., Cummins, E., Tchistiakova, L., Bloom, L., Paulsen, J., Gill, D., Cunningham, O., and Finlay, W. J. (2012) Fundamental characteristics of the immunoglobulin VH repertoire of chickens in comparison with those of humans, mice, and camelids. *J. Immunol.* **188,** 322–333
21. Andris-Widhopf, J., Rader, C., Steinberger, P., Fuller, R., and Barbas, C. F., 3rd. (2000) Methods for the generation of chicken monoclonal antibody fragments by phage display. *J. Immunol. Methods* **242,** 159–181
22. Ayyar, B. V., Hearty, S., and O'Kennedy, R. (2010) Highly sensitive recombinant antibodies capable of reliably differentiating heart-type fatty acid binding protein from noncardiac isoforms. *Anal. Biochem.* **407,** 165–171
23. McPhillips, T. M., McPhillips, S. E., Chiu, H. J., Cohen, A. E., Deacon, A. M., Ellis, P. J., Garman, E., Gonzalez, A., Sauter, N. K., Phizackerley, R. P., Soltis, S. M., and Kuhn, P. (2002) Blu-Ice and the distributed control system: software for data acquisition and instrument control at macromolecular crystallography beamlines. *J. Synchrotron Radiat.* **9,** 401–406
24. Kabsch, W. (2010) *Xds*. *Acta Crystallogr. D Biol. Crystallogr.* **66,** 125–132
25. Evans, P. (2006) Scaling and assessment of data quality. *Acta Crystallogr. D Biol. Crystallogr.* **62,** 72–82
26. Langer, G., Cohen, S. X., Lamzin, V. S., and Perrakis, A. (2008) Automated macromolecular model building for X-ray crystallography using ARP/wARP version 7. *Nat. Protoc.* **3,** 1171–1179
27. Emsley, P., Lohkamp, B., Scott, W. G., and Cowtan, K. (2010) Features and development of Coot. *Acta Crystallogr. D Biol. Crystallogr.* **66,** 486–501
28. Adams, P. D., Afonine, P. V., Bunkóczi, G., Chen, V. B., Davis, I. W., Echols, N., Headd, J. J., Hung, L. W., Kapral, G. J., Grosse-Kunstleve, R. W., McCoy, A. J., Moriarty, N. W., Oeffner, R., Read, R. J., Richardson, D. C., Richardson, J. S., Terwilliger, T. C., and Zwart, P. H. (2010) PHENIX: a comprehensive Python-based system for macromolecular structure solution. *Acta Crystallogr. D Biol. Crystallogr.* **66,** 213–221
29. Murshudov, G. N., Vagin, A. A., and Dodson, E. J. (1997) Refinement of macromolecular structures by the maximum-likelihood method. *Acta Crystallogr. D Biol. Crystallogr.* **53,** 240–255
30. Winn, M. D., Ballard, C. C., Cowtan, K. D., Dodson, E. J., Emsley, P., Evans, P. R., Keegan, R. M., Krissinel, E. B., Leslie, A. G., McCoy, A., McNicholas, S. J., Murshudov, G. N., Pannu, N. S., Potterton, E. A., Powell, H. R., Read, R. J., Vagin, A., and Wilson, K. S. (2011) Overview of the CCP4 suite and current developments. *Acta Crystallogr. D Biol. Crystallogr.* **67,** 235–242
31. Heinig, M., and Frishman, D. (2004) STRIDE: a web server for secondary structure assignment from known atomic coordinates of proteins. *Nucleic Acids Res.* **32,** W500–W502
32. Delano, W. L. (2002) *The PyMOL Molecular Graphics System*, Schrodinger, LLC, New York
33. Chen, V. B., Arendall, W. B., 3rd, Headd, J. J., Keedy, D. A., Immormino, R. M., Kapral, G. J., Murray, L. W., Richardson, J. S., and Richardson, D. C. (2010) MolProbity: all-atom structure validation for macromolecular crystallography. *Acta Crystallogr. D Biol. Crystallogr.* **66,** 12–21
34. Morea, V., Tramontano, A., Rustici, M., Chothia, C., and Lesk, A. M. (1998) Conformations of the third hypervariable region in the VH domain of immunoglobulins. *J. Mol. Biol.* **275,** 269–294
35. Shirai, H., Kidera, A., and Nakamura, H. (1996) Structural classification of CDR-H3 in antibodies. *FEBS Lett.* **399,** 1–8
36. North, B., Lehmann, A., and Dunbrack, R. L., Jr. (2011) A new clustering of antibody CDR loop conformations. *J. Mol. Biol.* **406,** 228–256
37. Wong, S. E., Sellers, B. D., and Jacobson, M. P. (2011) Effects of somatic mutations on CDR loop flexibility during affinity maturation. *Proteins* **79,** 821–829
38. Govaert, J., Pellis, M., Deschacht, N., Vincke, C., Conrath, K., Muyldermans, S., and Saerens, D. (2012) Dual beneficial effect of interloop disulfide bond for single domain antibody fragments. *J. Biol. Chem.* **287,** 1970–1979
39. Olsson, N., Wallin, S., James, P., Borrebaeck, C. A., and Wingren, C. (2012) Epitope-specificity of recombinant antibodies reveals promiscuous peptide-binding properties. *Protein Sci.* **21,** 1897–1910
40. Reynaud, C. A., Dahan, A., Anquez, V., and Weill, J. C. (1989) Somatic hyperconversion diversifies the single Vh gene of the chicken with a high incidence in the D region. *Cell* **59,** 171–183
41. Reynaud, C. A., Bertocci, B., Dahan, A., and Weill, J. C. (1994) Formation of the chicken B-cell repertoire: ontogenesis, regulation of Ig gene rearrangement, and diversification by gene conversion. *Adv. Immunol.* **57,** 353–378
42. Ratcliffe, M. J. (2006) Antibodies, immunoglobulin genes and the bursa of Fabricius in chicken B cell development. *Dev. Comp. Immunol.* **30,** 101–118
43. Hu, Z. Q., Li, H. P., Zhang, J. B., Huang, T., Liu, J. L., Xue, S., Wu, A. B., and Liao, Y. C. (2013) A phage-displayed chicken single-chain antibody fused to alkaline phosphatase detects *Fusarium* pathogens and their presence in cereal grains. *Anal. Chim. Acta* **764,** 84–92
44. McDonnell, B., Hearty, S., Finlay, W. J., and O'Kennedy, R. (2011) A high-affinity recombinant antibody permits rapid and sensitive direct detection of myeloperoxidase. *Anal. Biochem.* **410,** 1–6
45. Fitzgerald, J., Leonard, P., Darcy, E., Danaher, M., and O'Kennedy, R. (2011) Light-chain shuffling from an antigen-biased phage pool allows 185-fold improvement of an anti-halofuginone single-chain variable fragment. *Anal. Biochem.* **410,** 27–33
46. Bowes, T., Hanley, S. A., Liew, A., Eglon, M., Mashayekhi, K., O'Kennedy, R., Barry, F., Taylor, W. R., O'Brien, T., Griffin, M. D., Finlay, W. J., and Greiser, U. (2011) Developing cell-specific antibodies to endothelial progenitor cells using avian immune phage display technology. *J. Biomol. Screen* **16,** 744–754
47. Foord, A. J., Muller, J. D., Yu, M., Wang, L. F., and Heine, H. G. (2007) Production and application of recombinant antibodies to foot-and-mouth disease virus non-structural protein 3ABC. *J. Immunol. Methods* **321,** 142–151
48. Finlay, W. J., Shaw, I., Reilly, J. P., and Kane, M. (2006) Generation of high-affinity chicken single-chain Fv antibody fragments for measurement of the *Pseudo-nitzschia pungens* toxin domoic acid. *Appl. Environ. Microbiol.* **72,** 3343–3349
49. Foote, J., and Eisen, H. N. (1995) Kinetic and affinity limits on antibodies produced during immune responses. *Proc. Natl. Acad. Sci. U.S.A.* **92,** 1254–1256
50. Chailyan, A., Marcatili, P., Cirillo, D., and Tramontano, A. (2011) Structural repertoire of immunoglobulin lambda light chains. *Proteins* **79,** 1513–1524
51. Almagro, J. C., Raghunathan, G., Beil, E., Janecki, D. J., Chen, Q., Dinh, T., LaCombe, A., Connor, J., Ware, M., Kim, P. H., Swanson, R. V., and Fransson, J. (2012) Characterization of a high-affinity human antibody with a disulfide bridge in the third complementarity-determining region of the heavy chain. *J. Mol. Recognit.* **25,** 125–135
52. Wang, F., Ekiert, D. C., Ahmad, I., Yu, W., Zhang, Y., Bazirgan, O., Torkamani, A., Raudsepp, T., Mwangi, W., Criscitiello, M. F., Wilson, I. A., Schultz, P. G., and Smider, V. V. (2013) Reshaping antibody diversity. *Cell* **153,** 1379–1393
53. Abhinandan, K. R., and Martin, A. C. (2008) Analysis and improvements to Kabat and structurally correct numbering of antibody variable domains. *Mol. Immunol.* **45,** 3832–3839